Physiology and Pharmacology

Physiol Pharmacol 21 (2017) 331-342 **www.phypha.ir/ppj**

Original Article

Aerosol delivery of ferulic acid-loaded nanostructured lipid carriers: A promising treatment approach against the respiratory disorders

Parichehr Hassanzadeh[1]*, Elham Arbabi[2], Fatemeh Rostami[2], Fatemeh Atyabi[1], Rassoul Dinarvand[1]

1. Nanotechnology Research Center, Faculty of Pharmacy, Tehran University of Medical Sciences, Tehran, Iran
2. Research Institute for Gastroenterology and Liver Diseases, Shahid Beheshti University of Medical Sciences, Tehran, Iran

Abstract

Introduction: Treatment of lung diseases is one of the major healthcare challenges. Ferulic acid (FA), a phenolic compound with well-established antioxidant and anti-inflammatory properties, has shown promising therapeutic potential against the pulmonary disorders; however, low bioavailability may negatively affect its efficiency. This, prompted us to incorporate FA into the nanostructured lipid carriers (FA-NLCs) and evaluate the toxicity of this nanoformulation in human lung adenocarcinoma cell line (A549) and its suitability for pulmonary drug delivery.

Methods: FA-NLCs were prepared by high-pressure homogenization followed by assessment of the physicochemical properties of nanoparticles, *in vitro* release profile, aerosol characteristics, *in vitro* cytotoxicity, pharmacokinetic parameters and lung deposition of the nanoparticles after nebulization in Balb/c mice.

Results: Formation of FA-NLCs which exhibited a controlled release profile, was confirmed by scanning electron microscope and differential scanning calorimetry. FA-NLCs exhibited toxic effects on A549 cells for longer time periods as compared to FA solution. Following the aerosolization, suitable aerodynamic properties were obtained and FA-NLCs formulation provided significantly increased residence time and slower lung clearance for FA. Further confocal microscopy visualization confirmed the lung deposition of nanoparticles. Encapsulation of FA into the NLCs resulted in the improved pharmacokinetic parameters in plasma or lung tissue samples.

Conclusion: Application of the aerosolized FA-NLCs formulation which improves the pulmonary bioavailability of FA might result in the increased efficiency and reduced dosing frequency of this phytochemical. In this respect, development of inhalable nano-based drug delivery systems appears as a promising therapeutic approach against the lung disorders.

Keywords:
Ferulic acid;
Nanostructured lipid carriers;
Lung deposition;
Nebulization;
Balb/c mice

Received: 29 Apr 2017
Accepted: 11 Sep 2017

***Correspondence to:**
P. Hassanzadeh

Tel: +98-2166959095
Fax: +98-2166581558

Email:
p-hassanzadeh@razi.tums.ac.ir

Introduction

Respiratory disorders are among the most common healthcare problems worldwide (Ou et al., 2017). Over the last decade, the phenolic compounds have been shown as promising therapeutic candidates against the inflammatory disorders and oxidative

stress (Soobrattee et al., 2005). These compounds have also been represented as the potentiators of anticancer agents (Adhami et al., 2007). In this context, ferulic acid (4-hydroxy-3-methoxycinnamic acid, FA), a bioflavonoid with a wide variety of pharmacological activities (Gohil et al., 2012; Hassanzadeh et al., 2017a; Yang et al., 2015; Kim et al., 2013; Vashisth et al., 2015; Panwar et al., 2016) has shown preventive effects against the lung diseases (Lesca, 1983; Srinivasan et al., 2007). Meanwhile, low bioavailability and physiochemical instability (Ou and Kwok, 2004; Sohn and Oh, 2003) may negatively affect the efficiency of this valuable phytochemical. Over the last decades, eminent breakthroughs in the emerging field of nanotechnology have led to the development of novel theranostic strategies and protection of the encapsulated drugs or biomolecules against the excretion or metabolism within the body (Hassanzadeh et al., 2017b; Hassanzadeh et al., 2017c; Kubik et al., 2005). In recent years, lipid-based colloidal drug delivery systems including the nanostructured lipid carriers (NLCs) and solid lipid nanoparticles (SLNs) have been represented as alternative carrier systems to the polymeric nanoparticles, emulsions and liposomes. These biocompatible carriers protect the encapsulated active ingredients against the enzymatic degradation and are suitable for controlled drug release or targeted delivery (Müller, 2007). Moreover, they have shown better biodegradability and greater stability against the shear forces during the nebulization (Hitzman et al., 2006; Videira et al., 2002). Sterility and scale-up feasibility are some of the advantages of SLNs, however, application of these nanoparticles is associated with some limitations such as the limited drug-loading capacity and possibility of drug leakage during the storage or risk of gelation (Freitas and Müller, 1999; Müller et al., 1997; Müller, 2007). This has led to the development of a binary mixture of solid and liquid lipids, NLCs, with an imperfect matrix structure. Indeed, NLCs are a smarter generation of drug carriers with minimal drug expulsion during the storage, prolonged drug residence in the target organ, and high drug-loading capacity, stability and biocompatibility (Kumbhar and Pokharkar, 2013; Li et al., 2010; Müller, 2007). This background along with the advantages of inhalation drug delivery over the conventional routes of administration (Patton and Byron, 2007), prompted us to encapsulate FA into the NLCs (FA-NLCs) and provide a suitable nanoformulation for pulmonary drug delivery.

Materials and methods

Materials

Cell culture materials were all purchased from GIBCO/Invitrogen, Germany. Cetyl palmitate and Tween 80 were provided by Merck (Darmstadt, Germany) and other chemicals were purchased from Sigma Aldrich, Germany.

Animals

Male Balb/c mice weighing 22-25 g (Pasteur Institute, Iran) were randomly assigned and housed under central air conditioning (24±1 °C, humidity: 35-50%) and food pellets and water provided *ad libitum*. Animals were acclimated to the laboratory conditions for one week before the experiments. Five days before the nebulization studies, animals were trained by nebulizing water for 30 min in order to reduce discomfort during the nebulization. *In vivo* experiments were carried out in accordance with National Institutes of Health guidelines for the humane use of laboratory animals and approved by the local Ethics Committee.

Preparation of ferulic acid-loaded NLCs (FA-NLCs)

FA-NLCs were prepared by high-pressure homogenization (Beloqui et al., 2013) with some modifications. Briefly, the lipid phase (cetyl palmitate and oleic acid; 85:15 or 70:30) was prepared at 75 °C and then FA was added at 5, 10, 20, 40 or 100 % w/w. The aqueous phase was prepared at 75 °C by dispersing poloxamer 188 (0.5 or 1%, w/v) and Tween 80 (1 or 2%, w/v) in double-distilled water and was subsequently added to the lipid phase under high-speed stirring (Ultra Turrax T25, IKA, Germany) at 8000 rpm for 30s. The obtained pre-emulsion was subjected to high-pressure homogenization using a homogenizer (Micron LAB 40, Germany) at 500 bar and 75 °C for ten cycles. For further size reduction, the emulsion was sonicated using a probe sonicator (Ultra sonic, tecno-Gaz Tecna 6, Italy) at 70% amplitude for 2, 4, 10 or 15 min. The blank NLCs were prepared using the same procedure.

Assessment of the particle size, polydispersity index (PDI) and zeta potential (ZP) of FA-NLCs

NLCs dispersions were diluted by filtered deionized water to provide a suitable scattering intensity and then mean particle size and PDI (a measure of the width of particle size distribution) were analyzed at 25 °C by photon correlation spectroscopy (Zetasizer, Malvern Instruments, UK), a technique based on the dynamic laser light scattering due to the Brownian motion of the particles in a solution or suspension. ZP, the electrostatic potential on the surface of nanoparticles which reflects the physical stability of a colloidal system, was assessed by determination of the electrophoretic mobility (n=6).

Morphological assessment of FA-NLCs

Scanning electron microscope (KYKY-EM3200, China) was used to evaluate the shape of the lipid nanoparticles. In brief, the sample was mounted on the aluminium stub and coated with gold-palladium alloy in a Denton DV 502 vacuum evaporator at an accelerating voltage of 26 kV.

Entrapment efficiency (EE) and drug loading capacity (DL)

EE% and DL% of FA in NLC dispersion was determined by ultrafiltration method using the centrifugal filter tubes with a molecular weight cut-off (MWCO) of 10 kDa (Amicon Ultra, Millipore, Ireland). The 0.5 ml of FA-NLCs was centrifuged at 12000 rpm for 30 min and then FA content was analyzed by high-performance liquid chromatography (HPLC) using the Hitachi Model D-7000 (Merck, Darmstadt, Germany) system including a UV-Vis detector (Merck-Hitachi, L-4250, Germany) with C18 column (250×4.6 mm, 5 µm). The mobile phase contained methanol and 2% acetic acid (60:40 v/v) at a flow rate of 1 ml/min. For construction of the calibration curve, the serial dilutions of FA in methanol (2.5-250 µg/ml) were prepared and after determination of the absorbance, linear regression value of r^2 = 0.9995 was obtained. The peak absorption wavelength was recorded at 320 nm and the limit of detection and limit of quantification were obtained as 0.6 µg/ml and 1.58 µg/ml, respectively. EE% and DL% were determined as follows:

$$EE\% = \frac{\text{Total amount of FA} - \text{amount of free FA}}{\text{Total amount of FA}} \times 100$$

$$DL\% = \frac{\text{The amount of FA encapsulated in NLCs}}{\text{Total amount of NLCs}} \times 100$$

Differential scanning calorimetry (DSC)

Thermal analysis of pure FA, cetyl palmitate, freeze-dried FA-NLCs or blank NLCs was performed using the DSC apparatus (Mettler-Toledo, Switzerland). Each sample was placed in an aluminum pan and heated in the range of 10-240 °C (10 °C/min) under a nitrogen purge (50 ml/min). An empty aluminum pan was used as the reference and each experiment was carried out in triplicate.

Assessment of the *in vitro* release

The release profile of FA form NLCs was evaluated by dialysis membrane method (Yang et al., 2012). Briefly, 5 ml of FA-NLCs solution was transferred into a dialysis bag (MWCO: 10 kDa) which had been previously soaked in the release medium for 24 h. The dialysis bag was sealed at both ends, immersed into 250 ml of phosphate-buffered saline (PBS, pH 7.4) and stirred using a shaking incubator (Heidolph Unimax 1010, Germany) at 37 °C and 100 rpm. At defined time intervals, 0.5-ml samples were collected from the receptor phase, replaced with pre-warmed fresh PBS of an equal volume to maintain the sink condition and analyzed for FA content by HPLC. The percentage of dose released was plotted against the time and FA solution served as the control. Experiments were carried out in triplicate.

Storage stability

The freeze-dried samples were kept in the closed glass vials at 4 °C. At defined time intervals (1, 3 and 6 months), samples were re-suspended in filtered water and analyzed for the particle size, PDI, ZP, EE % and DL %. The results were expressed as the mean±SEM (n=6).

Aerosol characterization

Aerodynamic properties of NLCs were assessed using the eight-stage non-viable cascade impactor (Thermo Andersen Inc., Smyrna, GA, USA) equipped with filters. Each plate on the impactor was coated with 10% w/v pluronic L10 in ethanol in order to prevent particle bounce during the nebulization. Using Pari LC Star jet nebulizer, 3 ml of the optimized FA-NLCs formulation was nebulized into the impactor for 5 min at flow rate of 28.3 l/min. Afterwards, FA-

NLCs deposited on the throat, impactor stages and filter were collected after washing with 5 ml of tetrahydrofuran, centrifuged at 13,000 rpm for 20 min and the amount of FA was determined by HPLC. Mass median aerodynamic diameter (MMAD), geometric standard deviation (GSD) and fine particle fraction (FPF) were determined using Battelle software (Azarmi et al., 2006; Azarmi et al., 2008; Patlolla et al., 2010).

Cell culture

A549 cells were cultured in Dulbecco's modified Eagle's medium supplemented with 10 % fetal bovine serum (FBS), streptomycin sulfate (100 µg/ml), penicillin G sodium (100 U/ml) and amphotericin B (0.25 µg/ml) and incubated at 37 °C in a humidified atmosphere containing 5% CO_2. The culture media were changed every day and after 85-90% of confluency, cells were trypsinized by 0.05% trypsin and 0.53 mM EDTA solution and incubated for 5 min at 37 °C in humidified atmosphere with 5% CO_2. Trypsinization was stopped by adding 20% FBS followed by re-suspending, seeding and incubation. Experiments were carried out 72 h after seeding the cells with appropriate densities.

Assessment of FA-NLCs toxicity on the lung adenocarcinoma cell line

A549 cells were plated in 96-well microplates at a density of 1×10^4 cells/well. Following overnight incubation, cells were treated with 100, 250 and 500 µM of FA (Bouzaiene et al., 2015) or FA-NLCs (containing 100, 250 and 500 µM of FA), blank NLCs, or vehicle and then incubated in a 5% CO_2 incubator for 24, 48 or 72 h at 37 °C. Cell viability was assessed using MTT (3-[4,5-dimethylthiazol-2-yl]-2,5-diphenyl tetrazolium bromide) colorimetric assay which is based on the reduction of a tetrazolium salt by mitochondrial dehydrogenase in the viable cells (Carmichael et al., 1987). Cells were exposed to 0.5 mg/ml of MTT solution for 3 h at 37 °C and then the culture medium was carefully aspirated and replaced with 100 µl of DMSO and incubated at 37 °C in a humidified 5% CO_2-95% air mixture for 1 h. Then, the optical density of each well sample was determined at 570 nm using a microplate reader (Anthos 2020, Anthos Labtec Instruments, Austria). The cell viability was expressed as percentage of the untreated control cells (assuming the survival rate of 100%) and presented as mean±SEM of six independent experiments (n=6).

Aerosol drug delivery

The inexpose system (SCIREQ Scientific Respiratory Equipment Inc, Canada) including 12 ports peripherally located around a central delivery plenum was used for aerosol exposure to FA-NLCs or FA. Aerosols were produced by jet nebulizer using dry compressed air at a flow rate of 4.5 l/min. Animals restrained in the holders were placed in the inhalation chamber (SCIREQ, Canada) and the nose of each animal was exposed to the aerosol cloud for 30 min. The total deposited amount of inhaled FA (D) was calculated as follows; $D = C \times V \times DI \times T$. {C: the amount of FA collected in each port of the inhalation chamber (5.2 mg)/ total volume of the air withdrawn in 30 min [30 min × 4.5 liters/ 12 (number of ports) = 462.2 µg/l]; V: air volume inspired by the animal during one min (= 1.0 l min/kg for mice); DI: estimated deposition index (= 0.3 for mice) and T: duration of treatment (30 min)}.

The total deposited dose of FA during 30-min treatment was 4.16 mg/kg/day. Following the aerosol exposure, animals (n=6/group) were sacrificed with an overdose of halothane anesthesia at defined time intervals (0.5, 1, 2, 4, 6, 12 and 24 h) and then lung tissue samples were collected and stored at -80 °C. Upon the analysis, samples were processed as previously described (Patlolla et al., 2010). For further assessment of the lung deposition of FA-NLCs, mice were exposed to the fluorescent dye (DID-oil)-loaded NLCs for 30 min. After 0.5 and 4 h, lungs were removed, processed (Ichite et al., 2009) and the sections were observed using a confocal microscope (Leica DM6000).

Pharmacokinetic study

Area under the concentration-time curve (AUC), maximum concentration (C_{max}), time to reach C_{max} (T_{max}) and clearance (Cl) of FA in the plasma and lung were determined by non-compartmental analysis (WinNonLin, version 5.2.1, Pharsight Corporation, CA, USA) as previously described (Patlolla et al., 2010; Zhang et al., 2016).

Statistical analysis

T-test and analysis of variance (ANOVA) followed by

Table 1: Formulation design of FA-loaded NLCs

Formulation Codes	Solid/liquid lipids	Surfactant (w/v %)	FA/lipid (w/w%)	Sonication time (min)
FA-NLC1	Cetyl palmitate/oleic acid (85:15)	Poloxamer 188, Tween 80 (0.5, 1)	5	2
FA-NLC2	Cetyl palmitate/oleic acid (85:15)	Poloxamer 188, Tween 80 (0.5, 1)	5	4
FA-NLC3	Cetyl palmitate/oleic acid (85:15)	Poloxamer 188, Tween 80 (0.5, 1)	5	10
FA-NLC4	Cetyl palmitate/oleic acid (70:30)	Poloxamer 188, Tween 80 (1, 2)	5	15
FA-NLC5	Cetyl palmitate/oleic acid (70:30)	Poloxamer 188, Tween 80 (1, 2)	10	15
FA-NLC6	Cetyl palmitate/oleic acid (70:30)	Poloxamer 188, Tween 80 (1, 2)	20	15
FA-NLC7	Cetyl palmitate/oleic acid (70:30)	Poloxamer 188, Tween 80 (1, 2)	40	15
FA-NLC8	Cetyl palmitate/oleic acid (70:30)	Poloxamer 188, Tween 80 (1, 2)	100	15
Blank NLCs	Cetyl palmitate/oleic acid (70:30)	Poloxamer 188, Tween 80 (1, 2)	—	15

FA-NLCs: ferulic acid-loaded nanostructured lipid carriers

Table 2: Physichochemical properties of FA-loaded NLCs

Formulation codes	Particle size (nm)	PDI	ZP (mV)	EE (%)	DL (%)	DR after 48 h (%)
FA-NLC1	142.6 ± 7.4	0.37 ± 0.04	-23.7 ± 0.35	44.3 ± 3.2	1.42 ± 0.14	53.4 ± 3.5
FA-NLC2	129.7 ± 6.3	0.33 ± 0.07	-25.3 ± 0.47	47.9 ± 2.8	1.39 ± 0.07	51.3 ± 4.2
FA-NLC3	111.3 ± 8.5	0.27 ± 0.04	-23.9 ± 0.53	62.4 ± 3.7	1.57 ± 0.15	67.8 ± 3.8
FA-NLC4	69.7 ± 3.2	0.17 ± 0.06	-27.5 ± 0.38	93.5 ± 4.6	3.18± 0.07	82.3 ± 4.5
FA-NLC5	83.5 ± 3.7	0.15 ± 0.04	-24.3 ± 0.49	94.3 ± 5.2	6.24 ± 0.11	76.7 ± 4.3
FA-NLC6	90.7 ± 5.3	0.24 ± 0.08	-19.8 ± 0.24	88.6 ± 3.9	13.42± 2.3	74.5 ± 5.7
FA-NLC7	117.4 ± 9.6	0.18 ± 0.07	-26.6 ± 0.33	93.7 ± 5.3	31.17 ±1.7	62.3± 3.5
FA-NLC8	148.6 ± 7.4	0.25 ± 0.06	-24.9± 0.32	85.9 ± 4.7	45.72 ± 3.5	60.5 ± 2.8
Blank NLCs	54.9 ± 3.5	0.19 ± 0.05	-19.8 ± 0.28	–	–	–

Data are represented as mean±SEM (n=6).

(PDI: polydispersity index, ZP: zeta potential, EE: entrapment efficiency, DL: drug loading, DR: drug release, FA-NLCs: ferulic acid-loaded nanostructured lipid carriers)

Tukey's post hoc test were used for analysis of data which are presented as mean±SEM. Statistical significance was set at $P<0.05$.

Results

Characterization of FA-NLCs

FA-NLCs dispersions were successfully prepared by a modified high-pressure homogenization technique without signs of phase separation or color change during at least 1-month visual inspection. Using different ratios of solid and liquid lipids, FA and lipid, surfactants or sonication time, various FA-NLCs formulations were prepared (Tables 1 and 2). Application of the higher amount of oil lipid or surfactant resulted in the smaller particle size and higher entrapment efficiency (Table 2). Considering EE%, DL% and particle size, FA-NLCs7 (Table 2) was selected as the optimal formulation for further experimental procedures. According to the representative SEM image, nanoparticles were spherically shaped without pore on the surface (Fig. 1). In DSC thermograms, FA-NLCs displayed a melting peak at 45.9 °C (Fig. 2a), while, pure FA

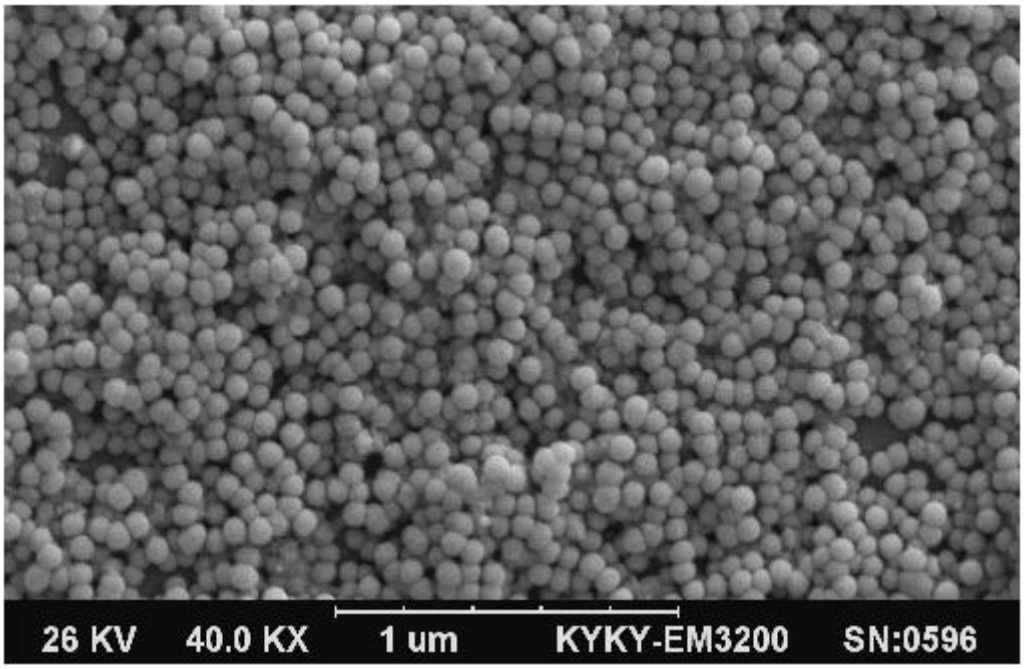

Fig.1. The representative scanning electron micrograph of FA-NLCs. Nanoparticles are spherically shaped without pore on the surface. FA-NLCs: ferulic acid-loaded nanostructured lipid carriers

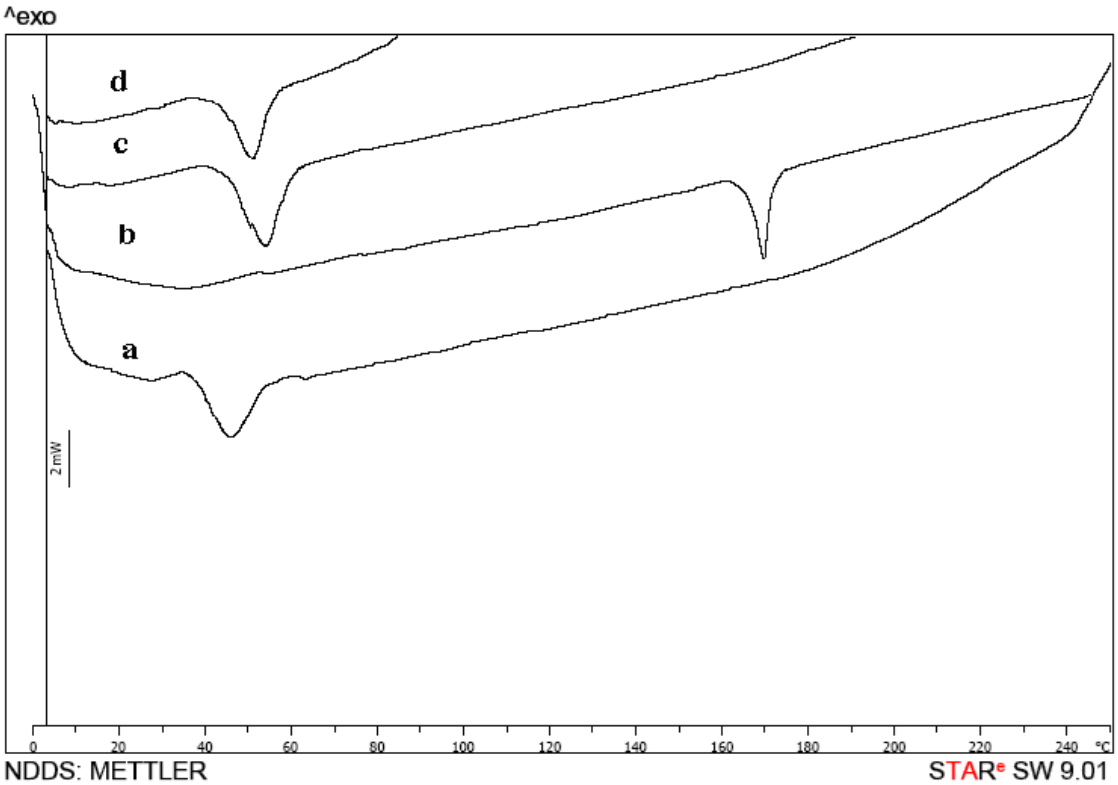

Fig.2. The overlaid DSC thermograms. a: FA-NLCs, b: FA, c: cetyl palmitate, d: blank NLCs. DSC: differential scanning calorimetry, FA-NLCs: ferulic acid-loaded nanostructured lipid carriers

showed a sharp endothermic peak at 174.2 °C (Fig. 2b). The melting peak of cetyl palmitate was observed at 55.7 °C (Fig. 2c) and blank NLCs showed a melting peak at 53.4 °C (Fig. 2d). Regarding the release profile, FA showed a controlled release pattern from FA-NLCs (Fig. 3). As shown in Table 3, the lyophilized nanoparticles remained stable at 4 °C without significant alterations in the particle size, PDI, ZP, EE% or DL% (P>0.05) during 6 months of storage.

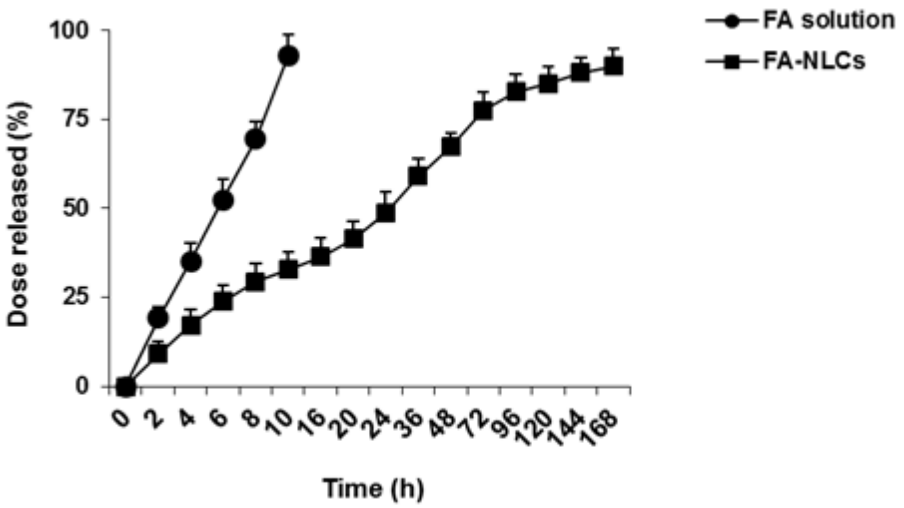

Fig.3. *In vitro* release profile of FA. A controlled release pattern of FA from FA-NLCs is observed. Data are expressed as the mean±SEM (n=3). FA-NLCs: ferulic acid-loaded nanostructured lipid carriers

Table 3: Stability profile of FA-NLCs

Initial				
Size	PDI	ZP	EE%	DL%
117.4±9.6	0.18±0.07	-26.6±0.3	93.7±5.3	31.2 ±1.7

1st Month				
Size	PDI	ZP	EE%	DL%
121.5±6.7	0.21±0.09	-26.3±0.6	94.3±5.4	31.4±1.5

3rd Month				
Size	PDI	ZP	EE%	DL%
119.7± 4.3	0.19±0.09	-25.7±0.9	91.8±4.3	29.8±0.9

6th Month				
Size	PDI	ZP	EE%	DL%
125.9± 7.2	0.22±0.07	-24.3±0.7	89.63±4.5	29.2±1.2

Data are represented as mean±SEM (n=6).
(PDI: polydispersity index, ZP: zeta potential, EE: entrapment efficiency, DL: drug loading, FA-NLCs: ferulic acid-loaded nanostructured lipid carriers)

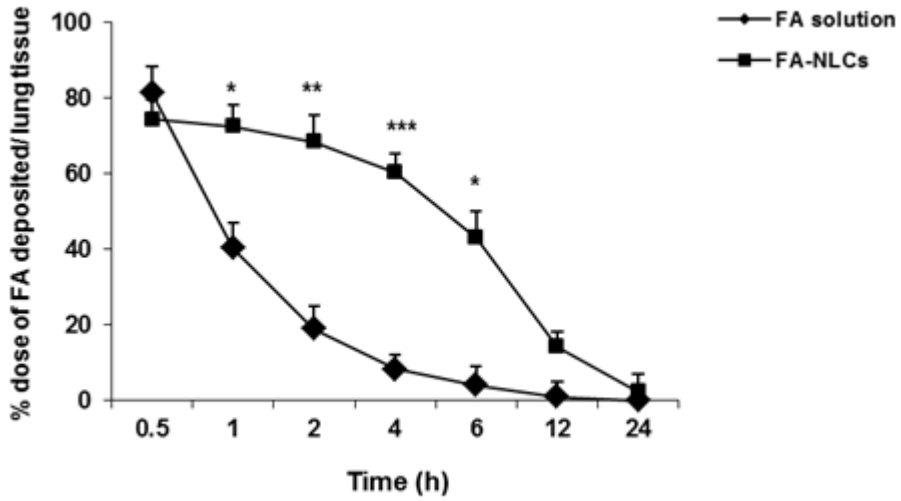

Fig.4. Lung deposition of FA-NLCs and FA solution following nebulization for 30 min in Balb/c mice. Data represent the mean±SEM (n=6). **P*<0.05, ***P*<0.01, ****P*<0.001 vs. FA solution. FA-NLCs: ferulic acid-loaded nanostructured lipid carriers

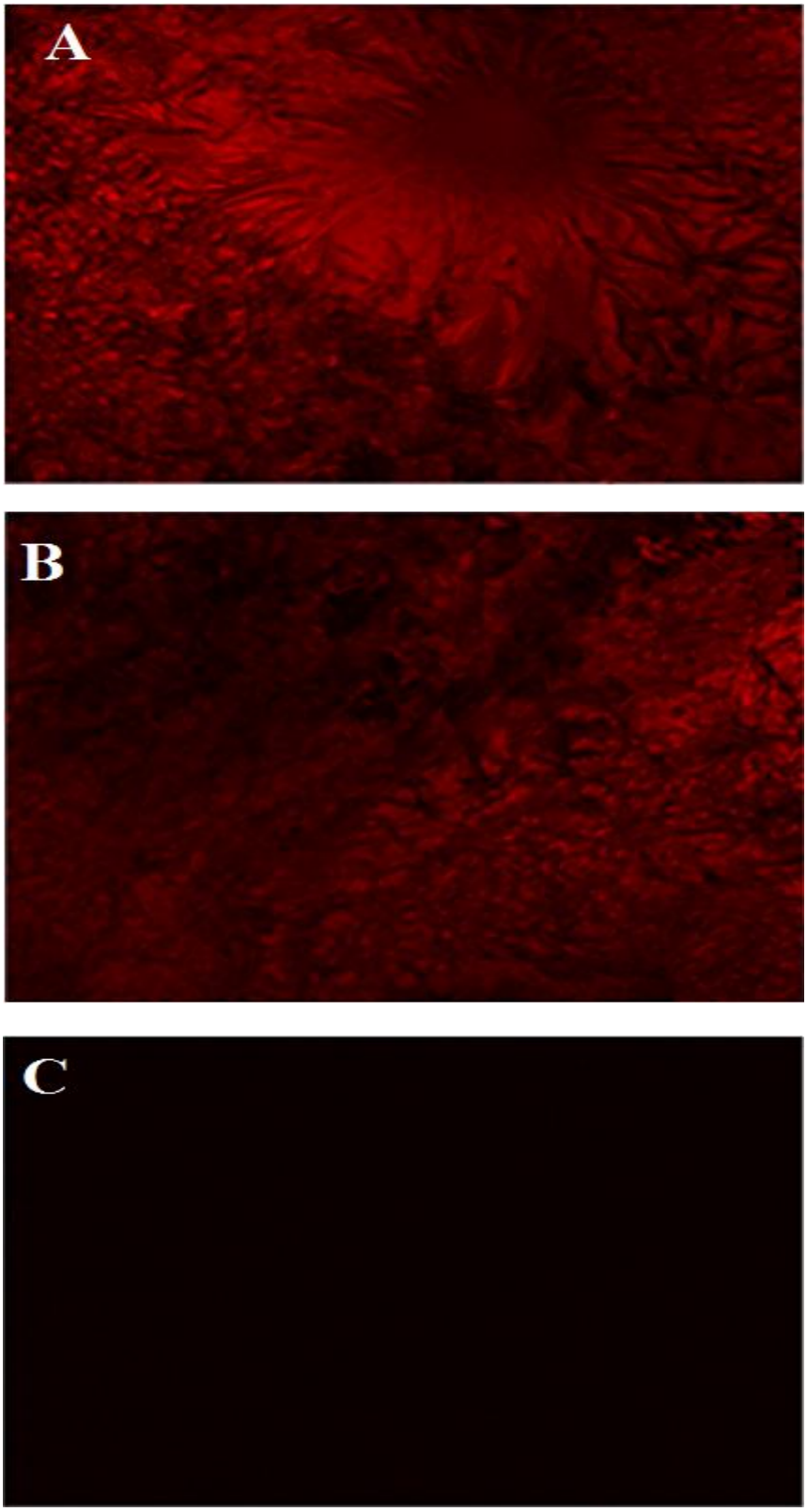

Fig.5. Lung disposition of fluorescent dye-loaded NLCs. 0.5 and 4 h after the nebulization of NLCs (A and B respectively), lungs were removed, processed and the fluorescent dye was visualized using a confocal microscope. C: untreated lung tissue. NLCs: nanostructured lipid carriers

MTT assay

As shown in Table 4, free FA (250 and 500 μM) reduced the cell viability only after 24 of incubation (P<0.001 *vs*. control), while, FA-NLCs (containing 100, 250 and 500 μM of FA) exhibited the cytotoxic effects for a longer period of time (P<0.001, P<0.01 *vs*. control). Blank NLCs did not affect the cell viability (P>0.05 *vs*. control).

Table 4: Cytotoxicity assays in A549 cell cultures

Groups	A (% of control)	B (% of control)	C (% of control)
Control	100	100	100
Vehicle	99.06 ±0.83	97.73 ±1.13	98.19 ±1.07
FA (100 µM)	93.29±0.98	95.11±2.37	94.46±2.23
FA (250 µM)	76.83±2.69 [a]	96.33±0.79	93.45±3.09
FA (500 µM)	68.49±1.76 [a]	95.48±1.26	95.13±2.48
FA-NLCs (100 µM)	74.11±3.17 [b]	79.07±3.29 [b]	70.29±2.77 [b]
FA-NLCs (250 µM)	70.35±4.32 [b]	62.85±2.44 [a]	65.13±4.82 [b]
FA-NLCs (500 µM)	61.43±2.25 [a]	58.12±3.05 [a]	50.47±2.17 [a]
Blank NLCs	95.72±2.43	93.42±3.16	95.13±1.79

A, B and C: cell viability after 24, 48 and 72 h of incubation, respectively. FA-NLCs 100, 250 and 500 µM are equivalent to 100, 250 and 500 µM of FA. As shown, FA-NLCs significantly reduced the cell viability for longer time periods. Data are expressed as the mean±SEM of six independent experiments for each treatment group. [a] $P<0.001$ and [b] $P<0.01$ *vs*. control.
(FA-NLCs: ferulic acid-loaded nanostructured lipid carriers)

Table 5: Pharmacokinetic parameters of FA and FA-NLCs in plasma and lung of Bulb-c mice after 30 min of neubilization

Parameter	Plasma		Lung	
	FA-NLCs	FA solution	FA-NLCs	FA solution
C_{max}	**21.53±2.13** [b]	**4.32±1.59**	**43.59±2.25** [c]	**11.28±0.92**
T_{max}	**3.94±0.13** [a]	**1.17±0.07**	**1.19±0.13** [a]	**0.32±0.05**
AUC_{0-t}	**162.17±7.73** [b]	**31.27±2.97**	**189.68±9.77** [b]	**53.19±1.65**
$AUC_{0-\infty}$	**169.43±5.69** [c]	**33.04±1.17**	**194.13±11.04** [b]	**60.24±4.15**
Cl	**1.52±0.08** [c]	**27.42±1.93**	**1.13±0.07** [c]	**23.19±1.46**

Data are expressed as mean±SEM (n=6). C_{max}: maximum concentration (µg/ml or µg/g tissue), T_{max}: time to reach C_{max} (h), AUC_{0-t}: area under the concentration-time curve from time 0 to the last measurable concentration, $AUC_{0-\infty}$: area under the concentration-time curve extrapolated to infinity (µg h/ml in plasma, µg h/g in lung), Cl: clearance (ml/h/kg), FA-NLCs: ferulic acid-loaded nanostructured lipid carriers. [a] $P< 0.05$, [b] $P<0.01$, [c] $P<0.001$ vs. FA solution

Aerosol characteristics

MMAD, GSD and FPF of FA-NLCs were obtained as follows: 1.53±0.11 µm, 1.4±0.08 and 82.3±5.7%, respectively. Data are represented as mean±SEM (n=6).

Lung deposition of FA-NLCs

After 30 min of nebulization of FA solution and FA-NLCs, 81.39±6.92% and 74.32±5.11% of FA was deposited in the lungs, respectively (Fig. 4). FA showed faster clearance in FA solution as compared to FA-NLCs in which an increased FA residence time and slower clearance was observed ($P<0.05$, $P<0.01$ and $P<0.001$ *vs*. FA solution). Further visualization of fluorescent dye-loaded NLCs confirmed the lung deposition of nanoparticles (Fig. 5).

Pharmacokinetic parameters

As shown in Table 5, encapsulation of FA into the NLCs resulted in higher C_{max} and AUC ($P<0.01$, $P<0.001$), greater T_{max} ($P<0.05$) and lower clearance ($P<0.001$) in plasma or lung tissue as compared to FA solution.

Discussion

Over the last decades, increasing research efforts

have been focused on the phytochemicals which have shown a wide variety of pharmacological activities. According to the beneficial effects of ferulic acid against the lung disorders (Lesca, 1983; Srinivasan et al., 2007), we have prepared FA-NLCs in order to improve the pharmacokinetic profile of FA and make the nanoformulation suitable for lung delivery. Assessment of the physichochemical properties of nanoparticles (Fig. 1, Tables 2 and 3) demonstrated the uniformity and spherical shape, narrow particle size distribution (indicating high homogeneity), suitable DL%, EE% (indicating the entrapment of FA into the lipid particle matrix), ZP (that might result in reduced particle aggregation) and stability profile indicating the appropriateness of preparation methods. Smaller particle size might result in the enhanced deposition of drug-entrapped particles in tracheo-bronchial and deep alveoli regions during the aerosolization process (Finlay, 2000) as well as the increased amount of drug absorbed due to the more homogenous drug distribution (Yang et al., 2008). In contrast to SLNs in which the aggregation or perikinetic flocculation may occur during the storage (Freitas and Müller, 1999; Müller, 1997; Müller, 2007), particles in highly-concentrated NLCs formed a network in fixed position (Fig. 1) that may not result in the collision of particles during the long-term storage. Thermal or crystalline behavior of the bulk materials, FA-NLCs and blank NLCs were determined by DSC (Fig. 2). The disappearance of sharp endothermic peak of pure FA in DSC thermogram of FA-NLCs indicates that FA is distributed in an amorphous status. The melting peaks of blank- or FA-NLCs shifted to the lower temperature indicating the transformation of bulk materials into the nanoparticulate forms. Depression of melting point may also be attributed to the small particle size, enhanced surface area of nanoparticles and less-ordered arrangement of NLCs (Siekmann and Westesen, 1994). In comparison to blank NLCs, FA-NLCs showed lower melting point that might be due to the incorporation of FA into the lipid matrix and enhancement of the defect levels in lipid crystal lattice.

A hyperbolic trend in the release profile (Fig. 3) indicates the controlled-release pattern of FA from NLCs which may be due to the partitioning of FA between the aqueous and lipid phases as well as the interactions between the surfactant-lipid or FA-lipid molecules. Furthermore, the prolonged release may be attributed to the diffusion of FA from the lipid core of NLCs. The delayed T_{max} of FA-NLCs (Table 5) also supports the sustained release of FA from the lipid matrix. This type of release by providing a constant concentration of FA for longer time period might be of therapeutic value.

MTT assay in A549 cell cultures (Table 4) revealed that FA-NLCs, but not free FA, exhibit cytotoxic effects for longer periods of time indicating the ability of this nanocarrier to provide a sustained concentration of FA due to the drug release in a controlled fashion (Fig. 3). Assessment of the aerodynamic properties of FA-NLCs (particularly MMAD of 1.53±0.11 µm µm) revealed the efficiency of the present nanocarrier system for drug delivery deep into the lung. As previously reported, aerosol particles with MMAD of 1-3 µm are optimal for pulmonary deposition throughout the respiratory zone (Byron, 1986; Beck-Broichsitter et al., 2011).

Regarding the lung deposition, nebulization of FA-NLCs resulted in slow elimination and improved lung deposition of FA (Figs. 4 and 5) that might be due to the controlled pattern of drug release (Fig. 3) and suitable composition and physichochemical properties of nanoparticles such as the small particle size (Tables 1 and 2). As previously reported, particles <260 nm deposit in the deep lung and escape the macrophage clearance (Lauweryns and Baert, 1977; Mansour et al., 2009; Patlolla et al., 2010). Indeed, the lipophilic outer surface of NLCs provides the possibility of nanoparticle adsorption to the surface of airway epithelium and overcoming the mucociliary lung transit (Schurch et al., 1990; Iyer et al., 2015). Improved lung deposition of FA following encapsulation into the NLCs has also been confirmed by the data demonstrating improved pharmacokinetic profile of FA as revealed by higher concentrations in both plasma and lung (Table 5) that might be due to the enhanced absorption and diffusion mobility of nanosized FA-loaded particles and their interaction with alveolar region or airway mucousal layer. Altogether, incorporation of FA into the NLCs is a promising approach to improve the bioavailability of this phenolic compound in both plasma and lung.

Conclusion

Inhalable FA-NLCs by providing a controlled release

pattern, slower clearance and higher concentration for FA that might result in enhanced efficiency and reduced dosing frequency, appears as a promising nanoformulation for lung drug delivery.

Acknowledgments

Authors wish to thank Prof. Hosnieh Tajerzadeh, Department of Pharmaceutics, Faculty of Pharmacy, Tehran University of Medical Sciences, Tehran, Iran, for helpful discussion.

Conflict of interest

None of the authors has any conflict of interest to disclose.

References

Adhami VM, Malik A, Zaman N, Sarfaraz S, Siddiqui IA, Syed DN, et al. Combined inhibitory effects of green tea polyphenols and selective cyclooxygenase-2 inhibitors on the growth of human prostate cancer cells both in vitro and in vivo. Clin Cancer Res 2007; 13: 1611-19.

Azarmi S, Tao X, Chen H, Wang Z, Finlay WH, Löbenberg R, et al. Formulation and cytotoxicity of doxorubicin nanoparticles carried by dry powder aerosol particles. Int J Pharm 2006; 319: 155-61.

Azarmi S, Roa WH, Lobenberg R. Targeted delivery of nanoparticles for the treatment of lung diseases. Adv Drug Deliv Rev 2008; 60: 863-75.

Beck-Broichsitter M, Schmehl T, Seeger W, Gessler T. Evaluating the controlled release properties of inhaled nanoparticles using isolated, perfused, and ventilated lung models. J Nanomater 2011; 2011: 1-16.

Beloqui A, Solinís MÁ, Gascón AR, del Pozo-Rodríguez A, des Rieux A, Préat V. Mechanism of transport of saquinavir-loaded nanostructured lipid carriers across the intestinal barrier. J Contr Rel 2013; 166: 115-23.

Bouzaiene NN, Jaziri SK, Kovacic H, Chekir-Ghedira L, Ghedira K, Luis J. The effects of caffeic, coumaric and ferulic acids on proliferation, superoxide production, adhesion and migration of human tumor cells in vitro. Eur J Pharmacol 2015; 766: 99-105.

Byron PR. Prediction of drug residence times in regions of the human respiratory tract following aerosol inhalation. J Pharm Sci 1986; 75: 433-38.

Carmichael J, DeGraff WG, Gazdar AF, Minna JD, Mitchell JB. Evaluation of a tetrazolium-based semiautomated colorimetric assay: assessment of chemosensitivity testing. Cancer Res 1987; 47: 936-42.

Finlay WH, Gehmlich MG. Inertial sizing of aerosol inhaled from two dry powder inhalers with realistic breath patterns versus constant flow rates. Int J Pharm 2000; 210: 83-95.

Freitas C, Müller RH. Correlation between long-term stability of solid lipid nanoparticles (SLNs) and crystallinity of the lipid phase. Eur J Pharm Biopharm 1999; 47: 125-32.

Gohil KJ, Kshirsagar SB, Sahane RS. Ferulic acid-A comprehensive pharmacology of an important bioflavonoid. Int J Pharm Sci Res 2012; 3: 700-10.

Hassanzadeh P, Arbabi E, Atyabi F, Dinarvand R. Ferulic acid exhibits antiepileptogenic effect and prevents oxidative stress and cognitive impairment in the kindling model of epilepsy. Life Sci 2017a; 179: 9-14.

Hassanzadeh P, Arbabi E, Atyabi F, Dinarvand R. Nerve growth factor-carbon nanotube complex exerts prolonged protective effects in an *in vitro* model of ischemic stroke. Life Sci 2017b; 179: 15-22.

Hassanzadeh P, Arbabi E, Atyabi F, Dinarvand R. Application of carbon nanotubes as the carriers of the cannabinoid, 2-arachidonoylglycerol: towards a novel treatment strategy in colitis. Life Sci 2017c; 179: 66-72.

Hitzman CJ, Elmquist WF, Wattenberg LW, Wiedmann TS. Development of a respirable, sustained release microcarrier for 5-fluorouracil I: in vitro assessment of liposomes, microspheres, and lipid coated nanoparticles. J Pharm Sci 2006; 95: 1114-26.

Ichite N, Chougule MB, Jackson T, Fulzele SV, Safe S, Singh M. Enhancement of docetaxel anticancer activity by a novel diindolylmethane compound in human non-small cell lung cancer. Clin Cancer Res 2009; 15: 543-52.

Iyer R, Hsia CCW, Nguyen KT. Nano-therapeutics for the lung: state-of-the-art and future perspectives. Curr Pharm Des 2015; 21: 5233-44.

Kim HJ, Ryu K, Kang JH, Choi AJ, Kim T, Oh JM. Anticancer activity of ferulic acid-inorganic nanohybrids synthesized via two different hybridization routes, reconstruction and exfoliation-reassembly. Sci World J 2013; 2013: 421967.

Kubik T, Bogunia-Kubik K, Sugisaka M. Nanotechnology on duty in medical applications. Curr Pharm Biotechnol 2005; 6: 17-33.

Kumbhar DD, Pokharkar VB. Engineering of a nanostructured lipid carrier for the poorly water-soluble drug, bicalutamide: physicochemical investigations. Colloids Surf A Physicochem Eng Asp 2013; 416: 32-42.

Lauweryns JM, Baert JH. Alveolar clearance and the role of the pulmonary lymphatics. Am Rev Respir Dis 1977; 115: 625-83.

Lesca P. Protective effects of ellagic acid and other plant phenols on benzo[a] pyrene-induced neoplasia in mice. Carcinogenesis 1983; 4: 1651-53.

Li F, Weng Y, Wang L, He H, Yang J, Tang X. The efficacy and safety of bufadienolides loaded nanostructured lipid carriers. Int J Pharm 2010; 393: 203-11.

Mansour HM, Rhee YS, Wu X. Nanomedicine in pulmonary delivery. Int J Nanomed 2009; 4: 299-319.

Müller RH, Rühl D, Runge S, Schulze-Forster K, Mehnert W. Cytotoxicity of solid lipid nanoparticles as a function of the lipid matrix and the surfactant. Pharm Res 1997; 14: 458-62.

Müller RH. Lipid nanoparticles: recent advances. Adv Drug

Deliv Rev 2007; 59: 375–76.

Ou S, Kwok KC. Ferulic acid: pharmaceutical functions, preparation and applications in foods. J Sci Food Agric 2004; 84:1261-9.

Ou X, Hua Y, Liu J, Gong C, Zhao W. Effect of high-flow nasal cannula oxygen therapy in adults with acute hypoxemic respiratory failure: a meta-analysis of randomized controlled trials. Can Med Assoc J 2017; 189: E260-E67.

Panwar R, Sharma AK, Kaloti M, Dutt D, Pruthi V. Characterization and anticancer potential of ferulic acid-loaded chitosan nanoparticles against ME-180 human cervical cancer cell lines. Appl Nanosci 2016; 6: 803-13.

Patlolla RR, Chougule M, Patel AR, Jackson T, Tata PN, Singh M. Formulation, characterization and pulmonary deposition of nebulized celecoxib encapsulated nanostructured lipid carriers. J Cont Rel 2010; 144: 233-41.

Patton JS, Byron PR. Inhaling medicines: delivering drugs to the body through the lungs. Nat Rev Drug Discov 2007; 6: 67-74.

Schurch S, Gehr P, Im Hof V, Geiser M, Green F. Surfactant displaces particles toward the epithelium in airways and alveoli. Respir Physiol 1990; 80: 17-32.

Siekmann B, Westesen K. Thermoanalysis of the recrystallization process of melt-homogenized glyceride nanoparticles. Colloids Surf B: Biointerfaces 1994; 3: 159-75.

Sohn YT, Oh JH. Characterization of physicochemical properties of ferulic acid. Arch Pharm Res 2003; 26: 1002-8.

Soobrattee MA, Neergheen VS, Luximon-Ramma A, Aruoma OI, Bahorun T. Phenolics as potential antioxidant therapeutic agents: mechanism and actions. Mutat Res 2005; 579: 200-13.

Srinivasan M, Sudheer AR, Menon VP. Ferulic acid: therapeutic potential through its antioxidant property. J Clin Biochem Nutr 2007; 40: 92-100.

Vashisth P, Sharma M, Nikhil K, Singh H, Panwar R, Pruthi PA, et al. Antiproliferative activity of ferulic acid-encapsulated electrospun PLGA/PEO nanofibers against MCF-7 human breast carcinoma cells. Biotech 2015; 5: 303-15.

Videira MA, Botelho MF, Santos AC, Gouveia LF, De Lima JJ, Almeida AJ. Lymphatic uptake of pulmonary delivered radiolabelled solid lipid nanoparticles. J Drug Target 2002; 10: 607-13.

Yang R, Zhang S, Kong D, Gao X, Zhao Y, Wang Z. Biodegradable polymercurcumin conjugate micelles enhance the loading and delivery of low potency curcumin. Pharm Res 2012; 29: 3512-25.

Yang W, Peters JI, Williams III RO. Inhaled nanoparticles – a current review. Int J Pharm 2008; 356: 239-47.

Yang GW, Jiang JS, Lu WQ. Ferulic acid exerts anti-angiogenic and anti-tumor activity by targeting fibroblast growth factor receptor 1-mediated angiogenesis. Int J Mol Sci 2015; 16: 24011-31.

Zhanga Y, Lia Z, Zhanga K, Yanga G, Wanga Z, Zhao J, et al. Ethyl oleate-containing nanostructured lipid carriers improve oral bioavailability of trans-ferulic acid ascompared with conventional solid lipid nanoparticles. Int J Pharma 2016; 511: 57-64.